Interference Mitigation Scheme by Antenna Selection in Device-to-Device Communication Underlaying Cellular Networks

Yuyang Wang[‡], Shi Jin[‡], Yiyang Ni[*], and Kai-Kit Wong[§]

[‡]National Mobile Communications Research Laboratory, Southeast University, Nanjing 210096, China

[*]Jiangsu Key Laboratory of Wireless Communication,
Nanjing University of Posts and Telecommunications, Nanjing 210003, China

[§]Department of Electronic and Electrical Engineering, University College London, United Kingdom

Email: seuradiowyy@gmail.com, jinshi@seu.edu.cn, niyy@njupt.edu.cn, kai-kit.wong@ucl.ac.uk

Abstract

In this paper, we investigate an interference mitigation scheme by antenna selection in device-to-device (D2D) communication underlaying downlink cellular networks. We first present the closed-form expression of the system achievable rate and its asymptotic behaviors at high signal-to-noise ratio (SNR) and the large antenna number scenarios. It is shown that the high SNR approximation increases with more antennas and higher ratio between the transmit SNR at the BS and the D2D transmitter. In addition, a tight approximation is derived for the rate and we reveal two thresholds for both the distance of the D2D link and the transmit SNR at the BS above which the underlaid D2D communication will degrade the system rate. We then particularize on the small cell setting where all users are closely located. In the small cell scenario, we show that the relationship between the distance of the D2D transmitting link and that of the D2D interfering link to the cellular user determines whether the D2D communication can enhance the system achievable rate. Numerical results are provided to verify these results.

Index Terms

Antenna selection, D2D, system spectral efficiency, achievable rate gain.

I. Introduction

Communications today with rich multimedia services pose a variety of stringent demands for quality-of-service (QoS) and high data rates. The scarcity of spectrum resources under the ever increasing user demand, however, has

A part of this paper has been presented at IEEE WCSP 2014 [1].

made it challenging to deliver high quality services via wireless communications, whereas existing technologies, e.g., multiple-input multiple-output (MIMO), orthogonal frequency-division multiplexing (OFDM) and etc. cannot meet the growing expectation [2–5]. Therefore, fifth generation wireless techniques have included device-to-device (D2D) communication technology which may potentially accommodate a much larger number and more diverse set of mobile devices [6]. In D2D communication, devices (or users) are capable of directly communicating with each other without going through the base station (BS). By reusing the time and frequency resources of cellular systems, D2D communications enhance spectrum utilization and improve cellular coverage [7].

However, due to the coexistence of the D2D link and the cellular link in the underlaid D2D communication, the mutual interference severely deteriorates the system performance, thus making interference management a critical issue which leads to a vast body of literature concerned. To name a few, [8] investigated interference coordination both in the uplink and downlink in the reuse mode and revealed that the D2D users can have gain although the cellular network is interference-limited. An interference mitigation scheme based on greedy coloring was lately designed in [9], according to the derived neighbor distance, to mitigate the interference among the D2D pairs with a guaranteed QoS. In [10], the authors devised a novel scheme by using the K-Means method to group the UEs into clusters and then optimized the frequency-hopping based interference mitigation scheme with a genetic algorithm. Also, [11] presented an interference cancellation mechanism by using some assisting information from the eNodeB to perform power control and thus avoid interference to cellular users while reusing the uplink spectrum. Later, [12–14] presented precoding to mitigate the interference introduced in D2D communication. Most recently, [15] exploited the D2D communication for developing a cooperative interference cancellation scheme.

In this paper, we propose an interference-mitigation based antenna selection scheme for D2D communication underlaying downlink cellular networks. We first derive a closed-form expression for the achievable rate and then analyze its asymptotic behaviors in the high signal-to-noise ratio (SNR) regime and the scenario when the number of antennas grows very large. For simpler rate expressions, we present a novel tight approximation. By using the approximation, we show two thresholds for the distance between D2D terminals and the BS transmit SNR, respectively, above which the D2D communication will degrade the system achievable rate. Then we study the small cell setting where users are closely located. For the small cells, we investigate the scenario with infinite antennas deployed for interference mitigation and then explore three cases with different relationship between the distances of the D2D transmitting link and the interfering link. It is shown that only when the distance of the D2D transmitting link is smaller than the interfering link may the system achievable rate be improved by D2D communication.

The rest of this paper is organized as follows. Section II introduces the model of D2D communication underlaying downlink cellular networks. In Section III, a detailed illustration of the interference mitigation antenna selection scheme is given and the performance of the scheme is characterized, by deriving a closed-form expression for the system achievable rate. A novel tight approximation is provided in Section III, which facilitates the subsequent analysis concerning the power control and antenna number design in the macro cell and small cell scenarios, respectively. Some numerical results are provided in Section V to verify the theoretical results. Section VI concludes

the paper. All of the main mathematical proofs can be found in the appendices.

Throughout this paper, we adopt the following notations. Vectors are represented as columns and are denoted by lowercase boldface letters while matrices are represented by uppercase boldface letters. The subscript $(\cdot)^H$ indicates the matrix conjugate transpose operation. Also, $\mathbb{E}\{\cdot\}$ represents expectation of a random entity, while $|\cdot|$ returns the absolute value of a scalar. $\|\cdot\|$ denotes the norm of a vector, and $\Pr(\cdot)$ gives the probability of an event.

II. System Model

Let us consider a D2D communication underlaying downlink cellular networks with M antennas at the BS as depicted in Fig. 1. Three single-antenna remote user equipments (UEs) are referred to as UE0, UE1 and UE2, respectively. UE0 represents the cellular UE served directly by the BS, while UE1 and UE2 constitute the D2D link. The link directly connecting the BS and UE0 is denoted as Link0 and the link from the D2D transmitter UE2 to D2D receiver UE1 is referred as Link1.

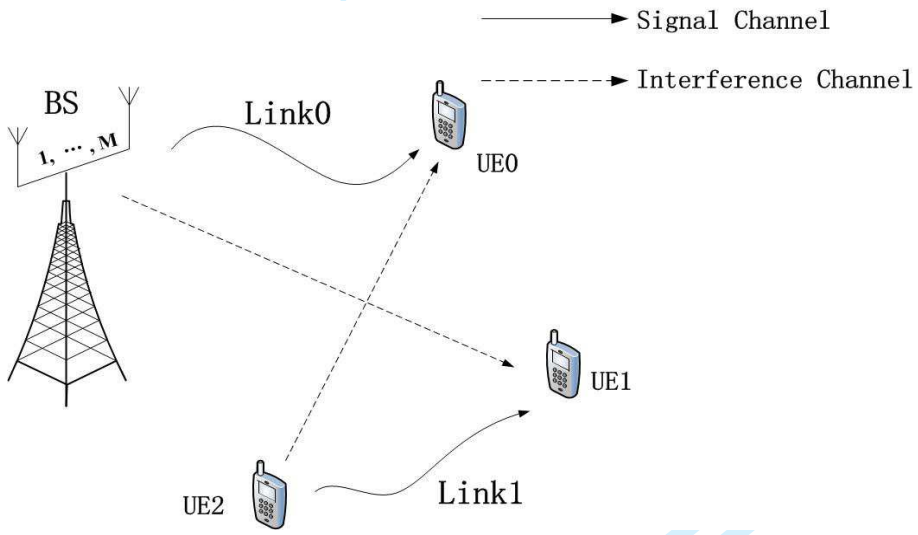

Fig. 1. D2D communication underlaying a downlink cellular network.

Assuming normalized transmitted symbols s_B and s_2, with $\mathbb{E}\{|s_i|^2\} = 1$ $(i = B, 2)$, the received symbol y_0 at the cellular user UE0 and y_1 at the D2D receiver UE1 can be written as

$$y_0 = \sqrt{\alpha_{B0} P_B}\mathbf{h}_{B0}^H \mathbf{w} s_B + \sqrt{\alpha_{20} P_2} h_{20} s_2 + n_0 \tag{1}$$

and

$$y_1 = \sqrt{\alpha_{B1} P_B}\mathbf{h}_{B1}^H \mathbf{w} s_B + \sqrt{\alpha_{21} P_2} h_{21} s_2 + n_1, \tag{2}$$

B refers to a BS.

where $\mathbf{h}_{Bj} \in \mathbb{C}^{M\times 1}$ $(j = 0, 1)$ is an M-dimensional vector characterizing the MIMO channel from the BS to either the cellular user or the D2D user, $\mathbf{w} \in \mathbb{C}^{M\times 1}$ is the transmit selection vector with $\mathbb{E}\{\|\mathbf{w}\|^2\} = 1$. Also, n_j models the additive Gaussian noise with zero mean and unit variance, α_{ij} characterizes the pathloss effect of the link between user equipment UEi and UEj and can be given by $\alpha_{ij} = D_{ij}^{-\eta}$, D_{ij} denotes the distance between UEi to UEj and η is the pathloss exponent. In particular, the pathloss exponent between the BS and UEs differs from that between the UEs due to the different propagation characteristics. In addition, with normalized noise here, we assume P_B and P_2 as the signal to noise ratio (SNR) of the BS and the D2D transmitter UE2, respectively.

According to the expressions in (1) and (2), the received signal-to-noise-plus-interference ratios (SINR) at UE0 and UE1 are, respectively, given by

$$\gamma_0 = \frac{\alpha_{B0} P_B |\mathbf{h}_{B0}^H \mathbf{w}|^2}{\alpha_{20} P_2 |h_{20}|^2 + 1} \tag{3}$$

and

$$\gamma_1 = \frac{\alpha_{21} P_2 |h_{21}|^2}{\alpha_{B1} P_B |\mathbf{h}_{B1}^H \mathbf{w}|^2 + 1}. \tag{4}$$

Hence, we can write the system achievable rate as

$$\mathcal{R} = \mathbb{E}\{\log_2(1 + \gamma_0)\} + \mathbb{E}\{\log_2(1 + \gamma_1)\}. \tag{5}$$

III. Analytical Results

In this section, we first present the interference mitigation antenna selection scheme and then derive the closed-form expression of system achievable rate. Based on that, we study the asymptotic behaviors of the achievable rate in the high SNR regime and the scenario when the antenna number becomes very large. In particular, we analyze the impacts of certain parameters on the high SNR approximation of the achievable rate.

A. Interference Mitigation Scheme by Antenna Selection

In the antenna selection scheme considered in this paper, the antenna selected for transmitting is the one from which the channel gain to UE1 is the minimum. The selected channel gain, denoted as $|\mathbf{h}_{B1}^H \mathbf{w}|^2$, can therefore be characterized as

$$|\mathbf{h}_{B1}^H \mathbf{w}|^2 = \min\{|h_{B1}^1|^2, |h_{B1}^2|^2, \ldots, |h_{B1}^M|^2\}, \tag{6}$$

where $|h_{B1}^k|^2$ is the channel gain from the kth antenna of the BS to UE1.

Since $|h_{B1}^k|^2 \sim \exp(1)$, we give its cumulative distribution function (CDF) as

$$F(x) = 1 - e^{-x}. \tag{7}$$

Hence, from (6) and (7), the CDF of $|\mathbf{h}_{B1}^H \mathbf{w}|^2$ can be given by

$$\Pr(|\mathbf{h}_{B1}^H \mathbf{w}|^2 < x) = 1 - \Pr(|h_{B1}|^2 > x) \Pr(|h_{B2}|^2 > x) \cdots \Pr(|h_{BM}|^2 > x). \tag{8}$$

After simple manipulations, we can obtain

$$\Pr(|\mathbf{h}_{B1}^H \mathbf{w}|^2 < x) = 1 - e^{-Mx}, \tag{9}$$

with its probability density function (PDF) given by

$$f(x) = Me^{-Mx}. \tag{10}$$

For UE0 in this scenario, we can easily get that $|\mathbf{h}_{B0}^H \mathbf{w}|^2 \sim \exp(1)$ because both $\mathbf{h}_{B0}$ and $\mathbf{w}$ are independently and identically distributed in the vector space and the vector $\mathbf{w}$ is a normalized vector with unit-norm.

It is also obvious that for $|h_{20}|^2$ and $|h_{21}|^2$, it holds that

$$|h_{20}|^2 \sim \exp(1) \tag{11}$$

and

$$|h_{21}|^2 \sim \exp(1). \tag{12}$$

Clearly, this antenna selection scheme requires perfect knowledge of the CSI at both the transmitter and receiver. In this paper, we primarily focus on the performance analysis assuming perfect CSI at both sides.

B. Achievable Rate

Before presenting the analysis, the following theorem will be useful for subsequent derivation.

Theorem 1. *For two random variables X, Y, $f(y) = Me^{-My}$, $N \sim \chi^2(2)$, $X = N/2$, and positive constants a and b, we have*

$$R(a,b,M) \triangleq \mathbb{E}\left\{\log_2\left(1 + \frac{X}{aY+b}\right)\right\} = \frac{M}{(M-a)\ln 2}\left(e^b E_1(b) - e^{\frac{bM}{a}} E_1\left(\frac{bM}{a}\right)\right), \tag{13}$$

where $E_1(z) = \int_z^\infty \frac{e^{-t}}{t} dt$ denotes the exponential integral function of the first order.

Proof. See Appendix A. □

1) General Expression: We first present a closed-form expression of the system achievable rate. According to (3)–(5) and (13), the system achievable rate $\mathcal{R}$ can be characterized as

$$\mathcal{R} = R\left(\frac{\alpha_{20}P_2}{\alpha_{B0}P_B}, \frac{1}{2\alpha_{B0}P_B}, 1\right) + R\left(\frac{\alpha_{B1}P_B}{\alpha_{21}P_2}, \frac{1}{2\alpha_{21}P_2}, M\right), \tag{14}$$

which can be further given by

$$\mathcal{R} = \frac{1}{\left(\frac{\alpha_{20}P_2}{\alpha_{B0}P_B} - 1\right)\ln 2}\left(e^{\frac{1}{2\alpha_{20}P_2}}E_1\left(\frac{1}{2\alpha_{20}P_2}\right) - e^{\frac{1}{2\alpha_{B0}P_B}}E_1\left(\frac{1}{2\alpha_{B0}P_B}\right)\right) + \frac{M}{\left(\frac{\alpha_{B1}P_B}{\alpha_{21}P_2} - M\right)\ln 2}\left(e^{\frac{M}{2\alpha_{B1}P_B}}E_1\left(\frac{M}{2\alpha_{B1}P_B}\right) - e^{\frac{1}{2\alpha_{21}P_2}}E_1\left(\frac{1}{2\alpha_{21}P_2}\right)\right). \quad (15)$$

We can observe from (15) that the achievable rate of UE1 varies proportionally with P_2 and inversely with P_B while the effect for UE0 is opposite. Hence, there is no clear relationship between the rate and the transmit SNR. Besides, no explicit observation concerning the impact of the number of antennas can be made due to the complexity of (15). In our analysis, we will mainly focus on two special cases including high SNR and the case where very large number of antennas are deployed, which shed light on the relevant parameters' impacts on achievable rate.

2) High SNR Scenario: We now analyze the asymptotic achievable rate when the transmit SNRs at the BS and UE2 grow very high, i.e., $P_B \to \infty$ and $P_2 \to \infty$, with fixed power ratio $C = P_B/P_2$.

Theorem 2. *For the antenna selection scheme, the achievable rate in high SNR regime is given by*

$$R_{HighSNR} = \frac{M}{\left(M - \frac{\alpha_{B1}P_B}{\alpha_{21}P_2}\right)\ln 2}\ln\frac{M\alpha_{21}P_2}{\alpha_{B1}P_B} + \frac{1}{\left(1 - \frac{\alpha_{20}P_2}{\alpha_{B0}P_B}\right)\ln 2}\ln\frac{\alpha_{B0}P_B}{\alpha_{20}P_2}. \quad (16)$$

Proof. See Appendix B. □

We can see that the high SNR approximation in (16) is only dependent on the transmit power ratio C, the number of antennas M and the pathloss factors. To further investigate it, considering $C \gg 1$, we can rewrite the high SNR approximation in (16) as

$$R_{HighSNR} = \frac{1}{\ln 2}\left(\frac{M}{M - \frac{\alpha_{B1}C}{\alpha_{21}}}\ln\frac{M\alpha_{21}}{\alpha_{B1}C} + \ln\frac{\alpha_{B0}C}{\alpha_{20}}\right), \quad (17)$$

which can be expanded as

$$R_{HighSNR} = \frac{1}{\ln 2}\left(\frac{\alpha_{21}M\ln\alpha_{21}M - \alpha_{B1}C\ln\alpha_{B1}C}{\alpha_{21}M - \alpha_{B1}C} + \ln\frac{\alpha_{B0}}{\alpha_{20}\alpha_{B1}}\right). \quad (18)$$

We define the function $f(x) \triangleq x\ln x$. Since $f''(x) = \frac{1}{x} > 0$, $f(x)$ is a convex function. Based on the property of convex functions, the asymptotic value in (18) increases with α_{21}, M as well as C. However, when $\alpha_{B1} \ll \alpha_{21}$, the effect of C on the high SNR approximation will be negligible. Moreover, the high SNR approximation varies proportionally with α_{B0} and inversely with α_{20}.

The above analysis in the high SNR regime demonstrates the disproportionally higher transmit SNR we have to sacrifice to achieve better system performance. However, a larger number of antennas can effectively break this limit and further enhance the system performance in the high SNR regime.

3) Analysis for Large M: We now particularize on the scenario where M is large, i.e., $M \to \infty$. We first exploit the fact that the exponential integral function of the first order $E_1(z)$ can be bounded by the following inequalities [16]:

$$\frac{1}{2}e^{-z}\ln\left(1+\frac{2}{z}\right) < E_1(z) < e^{-z}\ln\left(1+\frac{1}{z}\right). \tag{19}$$

For arbitrary z, it also holds that

$$\frac{1}{2}\ln\left(1+\frac{2}{z}\right) < e^{z}E_1(z) < \ln\left(1+\frac{1}{z}\right). \tag{20}$$

Therefore, it can be concluded that when z grows very large, $e^zE_1(z)$ can be bounded by

$$\lim_{z\to\infty}\frac{1}{2}\ln\left(1+\frac{2}{z}\right) < \lim_{z\to\infty} e^{z}E_1(z) < \lim_{z\to\infty}\ln\left(1+\frac{1}{z}\right). \tag{21}$$

Since both the upper and lower bounds of $e^zE_1(z)$ equal 0 with a very large z, we have

$$\lim_{z\to\infty} e^{z}E_1(z) = 0. \tag{22}$$

With the limit derived in (22) and according to the exact expression of the achievable rate in (15), in the large antenna number scenario, the achievable rate will approach to a constant value as

$$R_{LargeM} = \frac{1}{\left(\frac{\alpha_{20}P_2}{\alpha_{B0}P_B}-1\right)\ln 2}\left[e^{\frac{1}{2\alpha_{20}P_2}}E_1\left(\frac{1}{2\alpha_{20}P_2}\right) - e^{\frac{1}{2\alpha_{B0}P_B}}E_1\left(\frac{1}{2\alpha_{B0}P_B}\right)\right] + \frac{e^{\frac{1}{2\alpha_{21}P_2}}E_1\left(\frac{1}{2\alpha_{21}P_2}\right)}{\ln 2}. \tag{23}$$

The analysis above implies that the asymptotic behavior given in (23) will potentially restrict the application of this scheme in massive MIMO systems. In addition, it also suggests very slow improvement of the achievable rate when M is increased in a large scale, e.g., 100 or more [17, 18].

IV. Tight Approximations

The analysis in Section III provides the general achievable rate and the asymptotic achievable rate in two special scenarios. One is the high SNR regime and the other is the scenario with large number of antennas. However, these asymptotic results can only be applicable to a limited number of cases. As a consequence, for easier analysis, we derive a novel approximation, which is shown to be tight across the whole SNR regime. Based on this approximation, we first investigate the system achievable rate gain brought by D2D communication with different pathloss factors between the two D2D terminals and the transmit SNR at the BS. Then we study the interference-mitigation antenna selection scheme of D2D communication in the small cells.

A. Approximation Expressions

Although we have derived the asymptotic behaviors of the achievable rate, we still find it very difficult to discover the exact relationship between the relevant system cost parameters with the achievable rate, which is crucial to better

understand the antenna selection scheme and power control of the BS and the D2D transmitter. Therefore, in this subsection, we present a tight approximation of the achievable rate according to bracketing values of the inequality cited in (19), which helps obtain a simpler expression of the achievable rate for further analysis. When substituting the bounds in (20) as approximations into (13), we have two approximations given by

$$R(a,b,M) \approx \frac{M}{2(M-a)\ln 2} \ln \frac{bM+2M}{bM+2a} \tag{24}$$

and

$$R(a,b,M) \approx \frac{M}{(M-a)\ln 2} \ln \frac{bM+M}{bM+a}, \tag{25}$$

yielding the following approximations for the system achievable rate as

$$\mathcal{R} \approx \frac{M}{2\left(M-\frac{\alpha_{B1}P_B}{\alpha_{21}P_2}\right)\ln 2} \ln \frac{M+4\alpha_{21}P_2M}{M+4\alpha_{B1}P_B} + \frac{1}{2\left(1-\frac{\alpha_{20}P_2}{\alpha_{B0}P_B}\right)\ln 2} \ln \frac{1+4\alpha_{B0}P_B}{1+4\alpha_{20}P_2} \tag{26}$$

and

$$\mathcal{R} \approx \frac{M}{\left(M-\frac{\alpha_{B1}P_B}{\alpha_{21}P_2}\right)\ln 2} \ln \frac{M+2\alpha_{21}P_2M}{M+2\alpha_{B1}P_B} + \frac{1}{\left(1-\frac{\alpha_{20}P_2}{\alpha_{B0}P_B}\right)\ln 2} \ln \frac{1+2\alpha_{B0}P_B}{1+2\alpha_{20}P_2}. \tag{27}$$

We will see from the numerical results in Section V that the approximation in (27) is tight with the exact analytical result across the whole SNR regime while the approximation in (26) is not accurate. Thus for the following analysis, the approximation in (27) serves as a simplified expression of the analytical achievable rate.

B. System Achievable Rate Gain

Based on the approximation in (27), since it holds $P_B \gg P_2$, we can simplify the approximation as

$$\mathcal{R} \approx \frac{M}{\left(M-\frac{\alpha_{B1}P_B}{\alpha_{21}P_2}\right)\ln 2} \ln \frac{M+2\alpha_{21}P_2M}{M+2\alpha_{B1}P_B} + \frac{1}{\ln 2} \ln \frac{1+2\alpha_{B0}P_B}{1+2\alpha_{20}P_2}. \tag{28}$$

Thus, without D2D communication, that is, $P_2 = 0$, the system achievable rate is given by

$$\mathcal{R}\Big|_{P_2=0} \approx \frac{\ln(1+2\alpha_{B0}P_B)}{\ln 2}. \tag{29}$$

Based on the approximate achievable rate with and without D2D communication in (28) and (29) respectively, we define the following gain d as

$$d \triangleq \mathcal{R} - \mathcal{R}\Big|_{P_2=0}, \tag{30}$$

which can be given by

$$d \approx \frac{1}{\ln 2}\left(\frac{M}{M-\frac{\alpha_{B1}C}{\alpha_{21}}} \ln \frac{M+2M\alpha_{21}P_2}{M+2\alpha_{B1}P_B} - \ln(1+2\alpha_{20}P_2)\right), \tag{31}$$

and d in (31) represents the system achievable rate gain brought about by the D2D communication, evaluated by the difference between the approximation of the achievable rate with and without D2D communication.

Considering that d is a function of α_{21} and P_B, we first give its derivative for α_{21} and have

$$d'(\alpha_{21}) \approx \frac{1}{\ln 2} \frac{M\alpha_{B1}C}{(\alpha_{21}M - \alpha_{B1}C)^2} \left(\frac{2\alpha_{21}P_2(\alpha_{21}M - \alpha_{B1}C)}{\alpha_{B1}C(1+2\alpha_{21}P_2)} - \ln \frac{M + 2M\alpha_{21}P_2}{M + 2\alpha_{B1}P_2C} \right). \tag{32}$$

Since we only care about the polarity of this derivative, we then focus on the analysis of

$$\hat{d}'(\alpha_{21}) \triangleq \frac{2\alpha_{21}P_2(\alpha_{21}M - \alpha_{B1}C)}{\alpha_{B1}C(1+2\alpha_{21}P_2)} - \ln \frac{M + 2M\alpha_{21}P_2}{M + 2\alpha_{B1}P_2C}, \tag{33}$$

which can then be rewritten as

$$\hat{d}'(\alpha_{21}) = 2P_2(\alpha_{21}M - \alpha_{B1}C) \left(\frac{\alpha_{21}}{\alpha_{B1}C(1+2\alpha_{21}P_2)} - \frac{\ln(M + 2M\alpha_{21}P_2) - \ln(M + 2\alpha_{B1}P_2C)}{2P_2(\alpha_{21}M - \alpha_{B1}C)} \right). \tag{34}$$

Define the function $g(x) \triangleq \ln x$ which is a monotonically increasing concave function. Thus, when $M\alpha_{21} > \alpha_{B1}C$, we have

$$\frac{\ln(M + 2M\alpha_{21}P_2) - \ln(M + 2\alpha_{B1}P_2C)}{2P_2(\alpha_{21}M - \alpha_{B1}C)} < g'(x)|_{x=M+2\alpha_{B1}P_2C}, \tag{35}$$

where $g'(x)|_{x=M+2\alpha_{B1}P_2C} = \frac{1}{M+2\alpha_{B1}P_2C}$. For another function $h(\alpha_{21}) = \alpha_{21}/(\alpha_{B1}C(1+2\alpha_{21}P_2))$, we see that it is a monotonically increasing function of the pathloss factor α_{21}. With $\alpha_{21} > \frac{\alpha_{B1}C}{M}$, we have $h(\alpha_{21}) > h(\frac{\alpha_{B1}C}{M}) = \frac{1}{M+2\alpha_{B1}CP_2}$. As a consequence, we conclude that when $M\alpha_{21} > \alpha_{B1}C$, it holds $d'(\alpha_{21}) > 0$.

On the other hand, when $M\alpha_{21} < \alpha_{B1}C$, we have $h(\alpha_{21}) < \frac{1}{M+2\alpha_{B1}CP_2}$ and

$$\frac{\ln(M + 2M\alpha_{21}P_2) - \ln(M + 2\alpha_{B1}P_2C)}{2P_2(\alpha_{21}M - \alpha_{B1}C)} > g'(x)|_{x=M+2\alpha_{B1}P_2C} \tag{36}$$

with the result that it also holds $d'(\alpha_{21}) > 0$ when $M\alpha_{21} < \alpha_{B1}C$. The analysis reveals that $d(\alpha_{21})$ is a monotonically increasing function of α_{21}; that is, the gain of the system achievable rate can be enhanced by shortening the distance between the D2D terminals.

Furthermore, since we can see clearly that when α_{21} grows very large, that is, the distance between the D2D users is very small, the gain becomes

$$d(\alpha_{21}) \approx \frac{1}{\ln 2} \left(\ln \frac{M + 2M\alpha_{21}P_2}{M + 2\alpha_{B1}P_B} - \ln(1 + 2\alpha_{20}P_2) \right) > 0. \tag{37}$$

However, when the pathloss factor α_{21} becomes fairly small, the gain is simply

$$d(\alpha_{21}) \approx -\frac{\ln(1 + 2\alpha_{20}P_2)}{\ln 2} < 0. \tag{38}$$

When the interference from UE2 to the cellular user $\alpha_{20}P_2$ becomes very small (i.e., the distance D_{20} grows fairly large), even in the case when $\alpha_{21} \to \infty$, the achievable rate gain $d \simeq 0$. Since the gain function d is a monotonically increasing function of α_{21}, there does not exist a threshold for the D2D distance D_{21}. In this scenario, the underlaid

D2D transmission always outperforms the cellular networks concerning the system achievable rate.

However, when the interfering distance D_{20} is not large enough, the gain d falls below 0 when α_{21} grows large. This yields a threshold of α_{21} below which the gain becomes negative and with lower α_{21}, the achievable rate will be degraded by the D2D communication. However, when α_{21} transcends the threshold, greater gain can be obtained from the increased α_{21}. Since we have $\alpha_{21} = D_{21}^{-\eta}$, it can be seen that there exists a threshold D_{th} of the distance between the two D2D terminals, and only when $D_{21} < D_{th}$ can the D2D communication enhance the system achievable rate. This will be illustrated in Section V.

Similarly, for different BS transmit SNR, we can reformulate d in (31) as

$$d \approx \frac{1}{\ln 2}\left(\alpha_{21}P_2 M \frac{\ln(M + 2M\alpha_{21}P_2) - \ln(M + 2\alpha_{B1}P_B)}{\alpha_{21}P_2 M - \alpha_{B1}P_B} - \ln(1 + 2\alpha_{20}P_2)\right). \tag{39}$$

Since $g(x) = \ln x$ is a monotonically increasing concave function and based on its property, we see that d in (39) varies inversely with P_B. In particular, when P_B is very small, we have

$$d \approx \frac{1}{\ln 2}\left(\ln(1 + 2\alpha_{21}P_2) - \ln(1 + 2\alpha_{20}P_2)\right), \tag{40}$$

which is positive since we have $\alpha_{21} > \alpha_{20}$.

When P_B becomes very large, we have

$$d \approx -\frac{\ln(1 + 2\alpha_{20}P_2)}{\ln 2}. \tag{41}$$

Similar to the above analysis of α_{21}, we see that the interfering distance D_{20} determines whether there exists a threshold of P_B above which the D2D link will degrade the system achievable rate. Thus, in practical deployment, to guarantee larger system achievable rate underlaid by D2D, the BS should first compare the actual D2D terminal distance and the BS power with given thresholds to guarantee the enhancement of the system achievable rate.

C. Small Cell Scenario

In this subsection, we investigate this antenna selection scheme in the small cells of heterogeneous networks (HetNets), namely the femtocells or picocells and so on. In these environments, all users are closely located. This inevitably introduces more severe mutual interference, which could potentially be handled by the deployment of antennas for interference mitigation.

Based on the approximation in (28), in the small cells where α_{21} is not much larger than α_{B1}, we first assume a relatively small number of antennas deployed at the BS. Thus we have $M \ll \alpha_{B1}C/\alpha_{21}$, with the result that the achievable rate of UE1 is negligible, and the system achievable rate can be formulated by

$$\mathcal{R} \approx \frac{1}{\ln 2}\ln\frac{1 + 2\alpha_{B0}P_B}{1 + 2\alpha_{20}P_2}. \tag{42}$$

Comparing the system achievable rate (42) in small cell and that in (29) without D2D communication, we see that

in the highly congested user distribution of small cells with small number of antennas, the D2D link will degrade the system achievable rate. On one hand, the signal of the D2D transmitter is blended into the background signal from the BS and becomes undetectable due to a limited number of antennas. On the other hand, the cellular UE experiences considerable interference from the D2D transmitter.

However, when we provide a very large number of antennas in the small cell and in turn provide a fairly powerful interference mitigation mechanism for the D2D link, we can rewrite (28) into

$$\mathcal{R} \approx \frac{\ln(1+2\alpha_{B0}P_B)+\ln(1+2\alpha_{21}P_2)-\ln(1+2\alpha_{20}P_2)}{\ln 2}. \tag{43}$$

Then we can derive the difference between the system achievable rate in small cells with an infinite number of antennas in (43) and that without D2D communication in (29) as

$$d \approx \frac{\ln(1+2\alpha_{21}P_2)-\ln(1+2\alpha_{20}P_2)}{\ln 2}. \tag{44}$$

From the gain in (44), we see that in the small cells, the relationship between the pathloss factor of the D2D transmitting link α_{21} and the D2D interfering link to the cellular UE α_{20} determines whether the system rate can be elevated by D2D communication. When $\alpha_{21} > \alpha_{20}$, the rate with D2D communication can still transcend that without D2D in the large system scenario. Further when $\alpha_{21} < \alpha_{20}$, even with infinite antennas, the achievable rate with D2D is always lower than that without D2D. Particularly, when $\alpha_{21} = \alpha_{20}$, when very large number of antennas are deployed for interference mitigation, the system achievable rate equals that without D2D communication.

The scenario with D2D communication in small cells actually can be interpreted as an extension from the two-dimensional embedded cells to a three-dimensional communication system. Since interference between the different tiers are essential in the performance enhancement, when the traffic becomes increasingly congested, i.e., when the users stay much closer, the challenges posed by interference coordination become much more pronounced. Thus, we can see that it poses more stringent demand for the D2D communication in the small cells to guarantee improvement of the system achievable rate, that is, $\alpha_{21} > \alpha_{20}$ with very large number of antennas.

V. Numerical Results

Here, we compare the exact analytical result, high SNR and large antenna number behaviors and the two newly-derived approximations of the system achievable rate. We also give the relevant numerical results under the two scenarios of macro cells and small cells.

For the traditional macro cell analysis, the simulation parameters are given in Table I. We give different pathloss exponents $\eta_1 = 3.5$ for the BS-UE path and $\eta_2 = 4$ for the UE-UE path, respectively, due to the different antenna heights of BS and UEs. It should be noted that we randomly set the specific values of user distance D_{ij} just to better demonstrate our findings in the aforementioned work in the following numerical results. In a macrocell with a radius $r = 500$m, we choose the distance of D2D UEs as 40m which is smaller than the distances between others.

Fig. 2 depicts the Monte Carlo simulation result, the exact analytical result, the high SNR approximation and the two approximations in (26) and (27). It can be observed that the analytical system achievable rate tightly approaches the high SNR approximation. Moreover, it is seen that the approximation in (27) coincides well with the exact achievable rate, which facilitates much easier analysis. However, we also observe that the approximation in (26) is not tight enough despite its same tendency as that of the system achievable rate.

Figs. 3 and 4 reveal the relationship between the asymptotic achievable rate and the power ratio as well as with the number of antennas at high SNR. We simulate with $D_{21} \ll D_{20}$, i.e., $\alpha_{21} \gg \alpha_{20}$, which is the general case in the D2D communication in traditional macro cells and we can see from Fig. 3 that the high SNR approximation coincides with different transmit power ratio. On the contrary, Fig. 4 shows that the increase of the number of antennas can still efficiently elevate this high SNR approximation, as predicted in the previous analysis.

Fig. 5 illustrates the achievable rate against different numbers of antennas and shows its asymptotic behavior when the number of antennas becomes very large. We observe that the slope of the ergodic rate enhancement is sharp when M is relatively small. However, when M increases, the improvement rate slows down, thus making it unattractive to apply a large number of antennas for interference mitigation due to the limited gain brought about by the higher costs of a larger antenna array.

To better demonstrate the effect of our antenna selections scheme, Fig. 6 compares the system achievable rate without and with D2D communication for different number of antennas. First, it can be seen that in the traditional macrocells, D2D communication along with the antenna selection scheme can greatly boost the achievable rate but at high SNR, the underlaid D2D communication becomes less effective as demonstrated before.

For the small cell analysis, we summarize the parameters in Table II. With a much smaller cell size with radius $\hat{r} = 50$m, the distances between the users are also much smaller than the parameters in the macrocell. In addition, contrary to the macrocell case, the pathloss exponents of the BS-UE link and that of the UE-UE link are equal, due to the similar propagation characteristics as both BS and UEs are located inside, and with similarly low heights.

Figs. 7–8 demonstrate the existence of the threshold of D2D distance D_{21} and the transmit SNR at the BS, above which the D2D communication will lower the system achievable rate. From Fig. 7, we see that the system achievable rate declines with D_{21} and when the interference is not small enough, e.g., $D_{20} = 100, 80, 50$m, there apparently exists a threshold of D_{21} above which D2D communication degrades the system rate. In Fig. 8, the

TABLE I
SIMULATION PARAMETERS FOR THE MACRO CELL SCENARIO.

PARAMETERS	Value
Macro Cell Size $\mathcal{O}$	$\pi(500)^2$
Distance from BS to UE0 D_{B1}	200m
Distance from BS to UE1 D_{B0}	320m
Distance from UE2 to UE0 D_{21}	40m
Distance from UE2 to UE1 D_{20}	250m
Pathloss exponent between BS and UEs η_1	3.5
Pathloss exponent between UEs η_2	4

achievable rate increases with P_B. It can also be noted that the system achievable rate will be lowered when P_B grows over a certain value when the interference exists. However, from the results in the two figures, we see that when the interfering distance D_{20} becomes fairly large, i.e., $D_{20} = 200$m, there does not exist such a threshold of D_{21} and P_B above which the achievable rate drops. In this case, the D2D communication always outperforms the no-D2D case, as far as the system rate is concerned, even when D_{21} and P_B become large enough.

Fig. 9 plots the achievable rate with very large number of antennas (in the numerical results, we just simulate with the large antenna approximation in (23)) under different D_{21} and that without D2D communication. It is explicitly shown that when the number of antennas becomes infinite, the system achievable rate gain by D2D communication with infinite antennas is actually determined by the relationship between D_{21} and D_{20}. Moreover, only when $D_{21} < D_{20}$ can the system achievable rate be elevated by the D2D communication in the small cells. When $D_{21} \geq D_{20}$, even when sufficiently large number of antennas are deployed for interference mitigation, the system achievable rate with underlaid D2D will always fall below that without D2D.

VI. Conclusion

This paper investigated the performance of the D2D communication underlaying downlink cellular networks. We studied the achievable rate under the antenna selection scheme for interference mitigation. A closed-form expression of the achievable rate was derived and its asymptotic behaviors were explored at high SNR as well as for the case with large number of antennas. In addition, a tight approximation was proposed and we showed that there exists thresholds for the distance between the D2D terminals and the transmit SNR at the BS above which the D2D communication will degrade the achievable rate. The performance in the small cells was also studied subsequently based on the gain of the system rate brought by D2D communication. Numerical results reveal that in the macro cells, the achievable rate will grow much slower when more antennas are deployed. In the small cells, we show that whether D2D communication could bring gain to system achievable rate is solely dependent on the relationship between the distances of the D2D transmitting link D_{21} and the D2D interfering link D_{20}.

TABLE II
Simulation parameters for the small cell scenario.

PARAMETERS	Value
Small Cell Size $\hat{\mathcal{O}}$	$\pi(50)^2$
Distance from BS to UE0 D_{B0}	15m
Distance from BS to UE1 D_{B1}	30m
Pathloss exponent between BS and UEs η_1	4
Pathloss exponent between UEs η_2	4

APPENDIX A
PROOF OF THEOREM 1

Given the two random variables X, Y, $f(x) = Me^{-Mx}$, $N \sim \chi^2(2)$, $Y = N/2$, and positive constants a and b, we first derive the CDF of the random variable $Z = \frac{X}{aY+b}$ as

$$Pr(Z < z) = P(x < ayz + bz) = \int_0^\infty Me^{-(ayz+bz)}e^{-My}dy, \tag{45}$$

which equals

$$F(z) = 1 - \frac{Me^{-bz}}{az + M}. \tag{46}$$

Hence, the achievable rate of SINR z is equivalent to

$$\mathbb{E}\{\log_2(1+z)\} = \frac{1}{\ln 2}\int_0^\infty \frac{1-F(z)}{1+z}dz = \frac{1}{\ln 2}\int_0^\infty \frac{Me^{-bz}}{(az+M)(z+1)}dz. \tag{47}$$

We then separate the above expression into two parts as

$$\mathbb{E}\{\log_2(1+z)\} = \frac{1}{\ln 2}\int_0^\infty \frac{1}{a-M}\left(\frac{Me^{-bz}}{z+\frac{M}{a}} - \frac{Me^{-bz}}{z+1}\right)dz, \tag{48}$$

which gives the final result

$$\mathbb{E}\{\log_2\left(1+\frac{X}{aY+b}\right)\} = \frac{M}{(a-M)\ln 2}\left(e^{\frac{bM}{a}}E_1\left(\frac{bM}{a}\right) - e^b E_1(b)\right). \tag{49}$$

APPENDIX B
PROOF OF THEOREM 2

We use the following expansion of the exponential integral function $E_1(x)$ for derivation:

$$E_1(x) = -\gamma - \ln x - \sum_{k=0}^{\infty}\frac{(-x)^k}{kk!}. \tag{50}$$

Then, for positive x and by utilizing the Taylor series expansion of e^x, the last part of (50) becomes

$$\left|\sum_{k=1}^{\infty}\frac{(-x)^k}{kk!}\right| = \sum_{k=1}^{\infty}\frac{x^k}{kk!} < \sum_{k=1}^{\infty}\frac{x^k}{k!} = e^x - 1. \tag{51}$$

With the inequality in (51), we have

$$\lim_{x\to 0}\sum_{k=1}^{\infty}\frac{x^k}{kk!} \le \lim_{x\to 0} e^x - 1 = 0. \tag{52}$$

Because x is positive, we see from (52) that

$$\lim_{x\to 0}\sum_{k=1}^{\infty}\frac{x^k}{kk!} = 0 \tag{53}$$

and thus have

$$\lim_{x\to 0}\sum_{k=1}^{\infty}\frac{(-x)^k}{kk!}=0 \tag{54}$$

and

$$E_1(x)|_{x\to 0}\approx -\gamma-\ln x, \tag{55}$$

where $\gamma\approx 0.577$ is the Euler-Mascheroni constant.

We then substitute the asymptotic expansion in (55) to the two parts in (13), yielding the following two results respectively as

$$\lim_{b\to 0}R(a,b,M)=\frac{M}{(a-M)\ln 2}\left[e^{\frac{bM}{a}}\left(-\gamma-\ln\frac{bM}{a}\right)-e^{b}(-\gamma-\ln b)\right], \tag{56}$$

which can be further simplified as

$$\lim_{b\to 0}R(a,b,M)=\frac{M}{(a-M)\ln 2}\lim_{b\to 0}\left(e^{b}\ln b-e^{\frac{bM}{a}}\ln\frac{bM}{a}\right)=\frac{M}{(a-M)\ln 2}\ln\frac{a}{M}. \tag{57}$$

The final result can thus be characterized as

$$R_{HighSNR}=\frac{M}{\left(M-\frac{\alpha_{B1}P_B}{\alpha_{21}P_2}\right)\ln 2}\ln\frac{M\alpha_{21}P_2}{\alpha_{B1}P_B}+\frac{1}{\left(1-\frac{\alpha_{20}P_2}{\alpha_{B0}P_B}\right)\ln 2}\ln\frac{\alpha_{B0}P_B}{\alpha_{20}P_2}. \tag{58}$$

REFERENCES

[1] Y. Wang, S. Jin, Y. Ni, and K.-K. Wong, "Interference-mitigation based antenna selection scheme in device-to-device communication underlaying cellular networks," in *Proc. Wireless Commun. Signal Process.*, pp. 1–6, Oct. 2014.

[2] A. Osseiran, F. Boccardi, V. Braun, K. Kusume, P. Marsch, M. Maternia, O. Queseth, M. Schellmann, H. Schotten, H. Taoka, H. Tullberg, M. Uusitalo, B. Timus, and M. Fallgren, "Scenarios for 5G mobile and wireless communications: the vision of the METIS project," *IEEE Commun. Mag.*, vol. 52, pp. 26–35, May 2014.

[3] A. Gohil, H. Modi, and S. Patel, "5G technology of mobile communication: A survey," in *Proc. IEEE Int. Conf. on Intell. Syst. and Signal Process.*, pp. 288–292, Mar. 2013.

[4] C. Felita and M. Suryanegara, "5G key technologies: Identifying innovation opportunity," in *Proc. IEEE Int. Conf. on Quality in Research*, pp. 235–238, June 2013.

[5] J. Andrews, S. Buzzi, W. Choi, S. Hanly, A. Lozano, A. Soong, and J. Zhang, "What will 5G be?," *IEEE J. Sel. Areas Commun*, vol. 32, July 2014.

[6] L. Wei, R. Q. Hu, Y. Qian, and G. Wu, "Enable device-to-device communications underlaying cellular networks: challenges and research aspects," *IEEE Commun. Mag.*, vol. 52, pp. 90–96, June 2014.

[7] M. Hasan, E. Hossain, and D. I. Kim, "Resource allocation under channel uncertainties for relay-aided device-

to-device communication underlaying LTE-A cellular networks," *IEEE Trans. Wireless Commun.*, vol. 13, pp. 2322–2338, Apr. 2014.

[8] K. Doppler, M. Rinne, C. Wijting, C. Ribeiro, and K. Hugl, "Device-to-device communication as an underlay to LTE-advanced networks," *IEEE Commun. Mag.*, vol. 47, pp. 42–49, Dec 2009.

[9] Y. Xu, Y. Liu, K. Yang, D. Li, and Q. Luo, "Interference mitigation scheme for device-to-device communication with QoS constraint," in *Proc. IEEE PIMRC*, pp. 1784–1788, Sept. 2013.

[10] Y.-H. Lee, H.-W. Tseng, C.-Y. Lo, Y.-G. Jan, L.-P. Chin, T.-C. Song, and H.-I. Hsu, "Using genetic algorithm with frequency hopping in device to device communication (D2DC) interference mitigation," in *Proc. IEEE Int. Symp. on Intell. Signal Process. and Commun. Syst.*, pp. 201–206, Nov. 2012.

[11] S. Xu, H. Wang, T. Chen, Q. Huang, and T. Peng, "Effective interference cancellation scheme for device-to-device communication underlaying cellular networks," in *Proc. IEEE Veh. Technol. Conf.*, pp. 1–5, Sept. 2010.

[12] W. Xu, L. Liang, H. Zhang, S. Jin, J. Li, and M. Lei, "Performance enhanced transmission in device-to-device communications: Beamforming or interference cancellation?," in *Proc. IEEE Globecom*, pp. 4296–4301, Dec. 2012.

[13] W. Fu, R. Yao, F. Gao, J. Li, and M. Lei, "Robust null-space based interference avoiding scheme for D2D communication underlaying cellular networks," in *Proc. IEEE WCNC*, pp. 4158–4162, Apr. 2013.

[14] H. Tang, C. Zhu, and Z. Ding, "Cooperative MIMO precoding for D2D underlay in cellular networks," in *Proc. IEEE ICC*, pp. 5517–5521, June 2013.

[15] R. Tanbourgi, H. Jakel, and F. Jondral, "Cooperative interference cancellation using device-to-device communications," *IEEE Commun. Mag.*, vol. 52, pp. 118–124, June 2014.

[16] M. Abramowitz and I. A. Stegun, eds., *Handbook of Mathematical Functions with Formulas, Graphs, and Mathematical Tables*. Dover Publications, 1964.

[17] E. Larsson, O. Edfors, F. Tufvesson, and T. Marzetta, "Massive MIMO for next generation wireless systems," *IEEE Commun. Mag.*, vol. 52, pp. 186–195, Feb. 2014.

[18] W. Liu, S. Han, C. Yang, and C. Sun, "Massive MIMO or small cell network: Who is more energy efficient?," in *Proc. IEEE WCNC Workshops*, pp. 24–29, Apr. 2013.

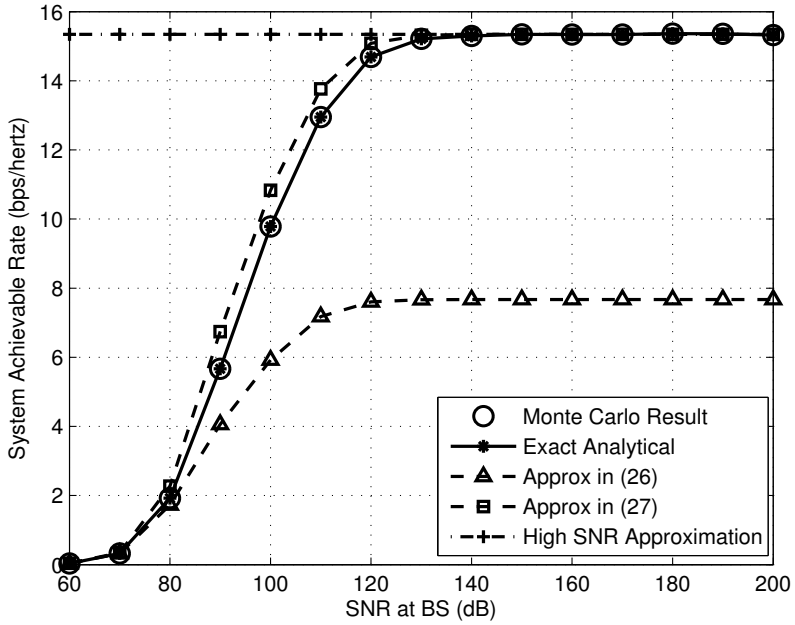

Fig. 2. Comparison of the exact analytical result, the high SNR approximation, the Monte-Carlo simulation result and the two new approximations derived in (26) and (27) with $P_B/P_2 = 100, M = 4$.

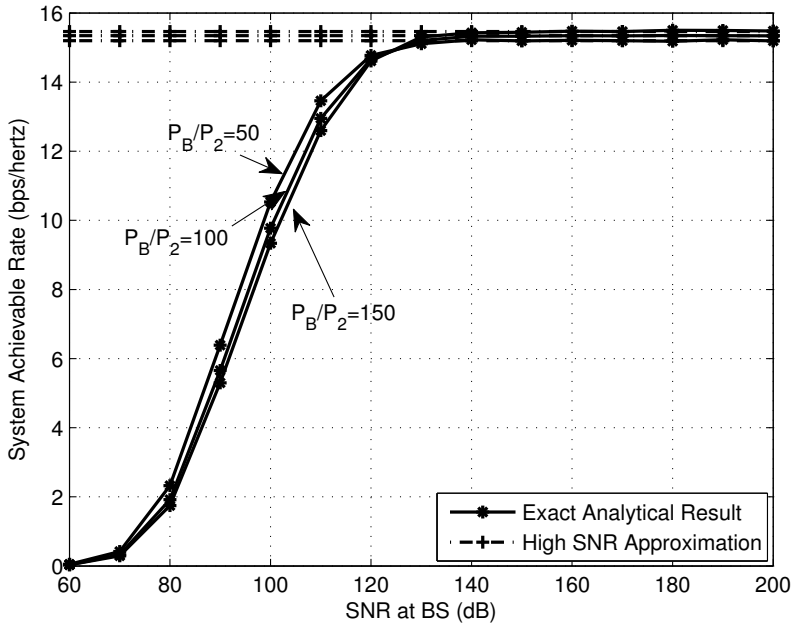

Fig. 3. Comparison of the high SNR approximations with different power ratio P_B/P_2.

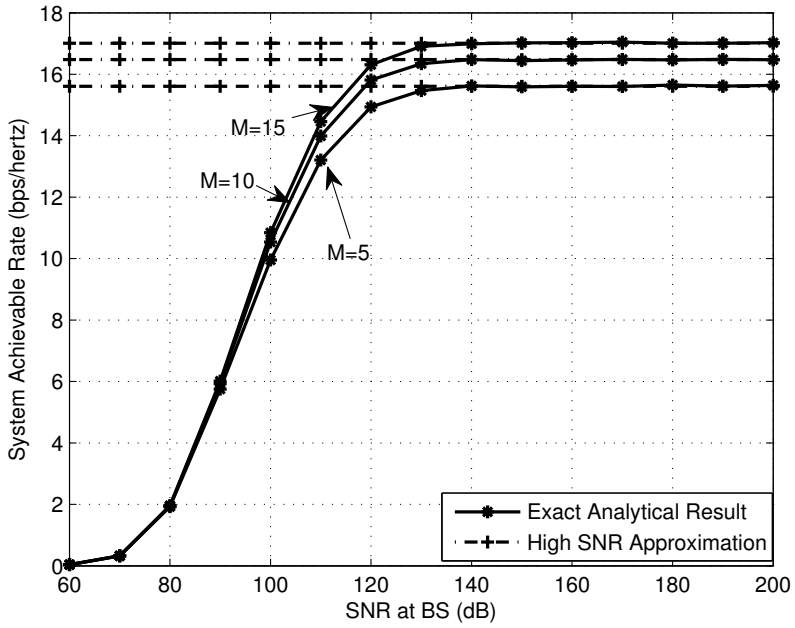

Fig. 4. Comparison of the high SNR approximations with different number of antennas M, $P_B/P_2 = 40$.

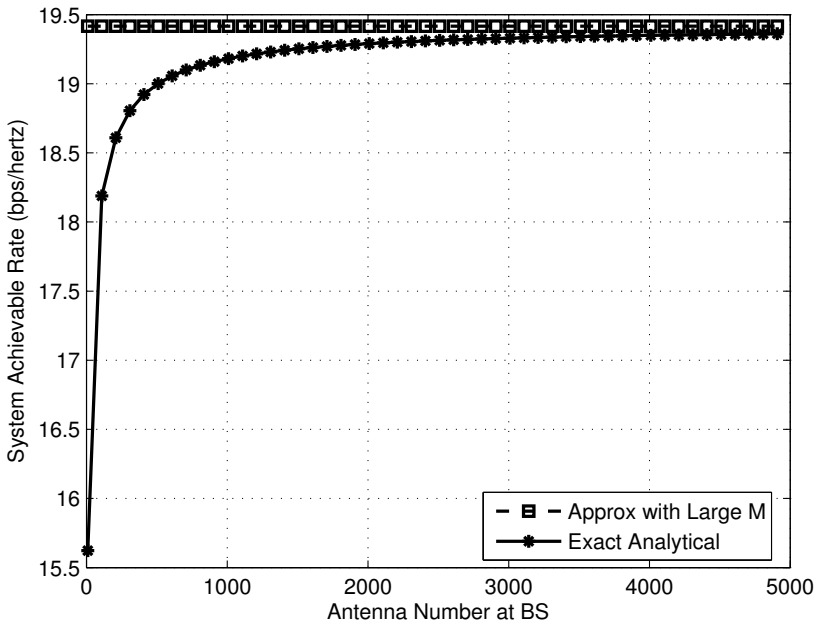

Fig. 5. System Achievable rate with different M for $P_B = 120$dB and $P_2 = 100$dB.

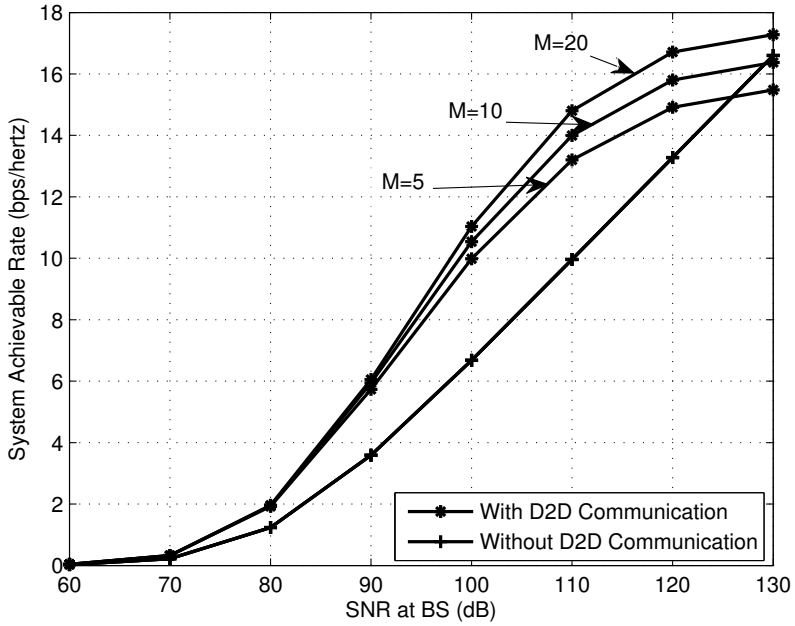

Fig. 6. Comparison of the system achievable rate with and without D2D communication. $P_B/P_2 = 100$.

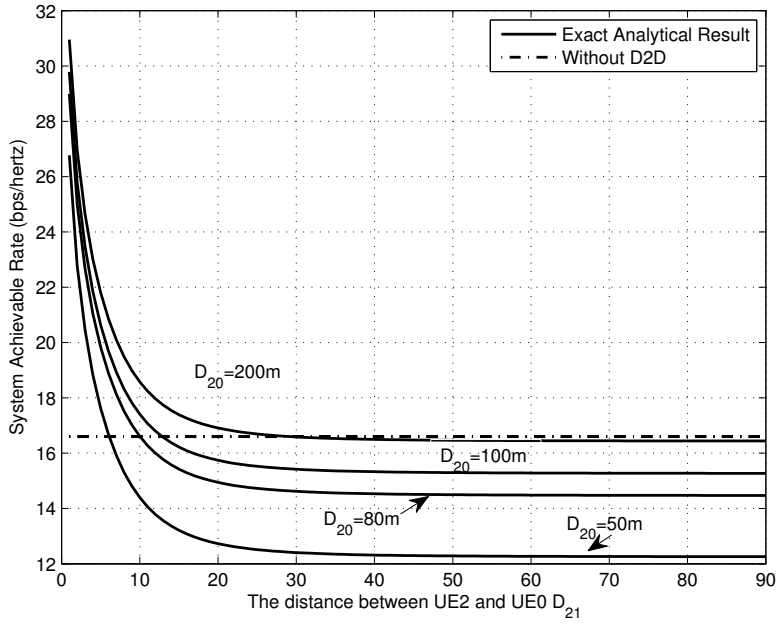

Fig. 7. Illustration of the threshold of D2D link distance D_{21} for the achievable rate gain, with different interfering distance D_{20}. $P_2 = 80$dB.

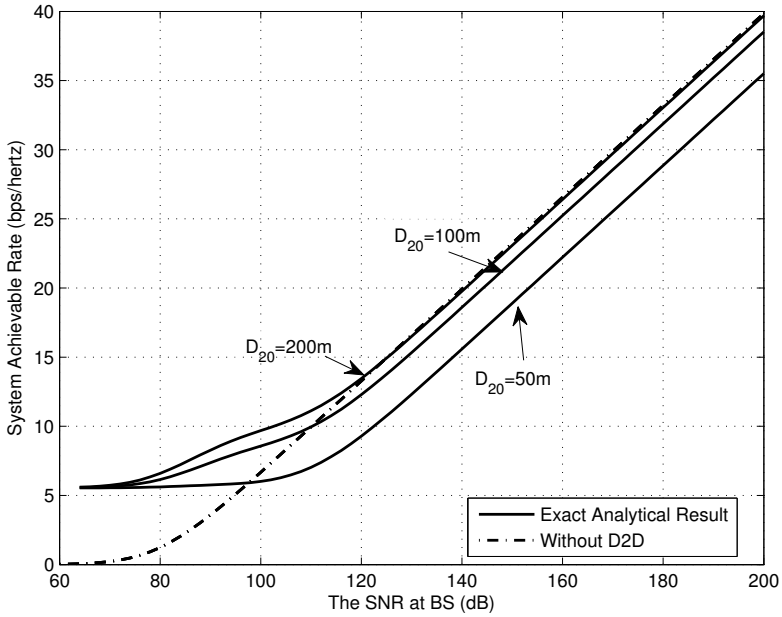

Fig. 8. Illustration of the threshold of transmit SNR at BS for the achievable rate gain, with different interfering distance D_{20}. $P_2 = 80$dB.

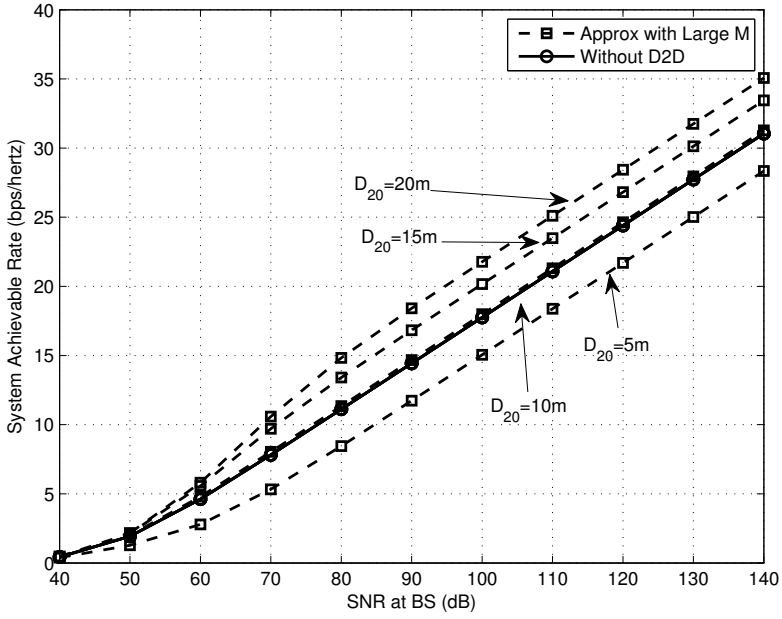

Fig. 9. Comparison of the system achievable rate with different D_{20}, with very large number of antennas deployed. $P_B/P_2 = 100$. $D_{21} = 10$m